# A UNILATERAL RF COIL FOR MR-SCINTIMAMMOGRAPHY

**S. Ha[1], M. J. Hamamura[1], W. W. Roeck[1], and O. Nalcioglu[1]**
[1]University of California Irvine, Irvine, California, United States

## Introduction

Although x-ray mammography is very sensitive in detecting early breast cancer, it does not work well in women who have dense breasts, breast implants, or scar tissues. In contrast MRI has been proven to be the most sensitive imaging modality in delineating tumor extent and detecting multifocal or multi centric diseases [1]. Many studies have indicated that preoperative MRI is useful in local staging for surgical planning, especially for patients with lobular cancer [2]. However, the low specificity of MRI, despite its high sensitivity, may lead to many unnecessary biopsies or over-treatment. Scintimammography (SMM) can be a tool to supplement MRI for improving the diagnostic specificity in breast cancer imaging [3]. The purpose of the present study was to evaluate the feasibility of operation of combination of MR breast coil and CZT detectors in a high field MRI magnet.

## Methods

**RF coil**: The proposed RF coil was designed for use in conjunction scintigraphic imaging for the unilateral breast imaging. As such it should have the best image quality, including good SNR and homogeneity within the region of interest in spite of the geometrical limitation that detectors for SMM imaging should be located in the space between the top and bottom plates of the coil frame. To meet these criteria, the mechanical structure of the coil (12cm height, 18cm width, and 15cm length) was designed as a square box with an opening for unilateral breast imaging (Fig 1). The coil has top to bottom spacing high enough to accommodate the height of the CZT detector/collimator of single photon mammography. The basic geometry of the breast coil comprised of four circular loops.

Fig.1: Experimental setup of breast array coil and RF shielding blocks covering CZT detectors. (a) Top view. Two RF shielding blocks were inserted in the opening of RF coil near a cylindrical phantom. (b) Side view.

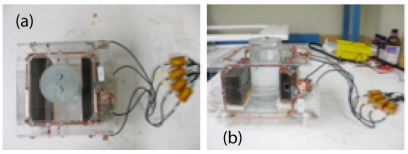


**CZT detector**: Each pixellated CZT module from Gamma Medica-Ideas, Inc. measures 2.54 cm x 2.54 cm and consists of 16 x 16 pixels with a 1.59 mm pixel pitch. Figure 2 shows the detector module. CZT detector module was set in an RF shielded box to minimize mutual interference of the two different imaging systems. The detector box was covered by a copper mesh fabric that has 40.3dB RF attenuation at 170MHz (4T MR system) with dimensions of 4cm height, 8cm width, and 2cm length.

Fig.2 (a) 2.54 cm x 2.54 cm, 16x16 pixel CZT module developed by Gamma Medica-Ideas, Inc. for nuclear medicine spectroscopic imaging. (b) Integrated CZT detector with data reconstruction cable assay with RF radiation shield.

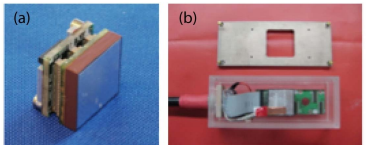


**Simulation and Experiments**: To investigate the $H_1$ magnetic field variation of the breast array coil while the CZT detectors are moved inside the breast array coil, boxes covered by copper mesh on the CZT detector modules were regarded as perfect conductive boxes in the simulation (Fig.3) (SEMCAD X Ver. 14.2.1 Schmid & Partner Engineering AG, Zürich, Switzerland). In order to estimate the variation of the resonance frequency of the breast array coil while CZT detectors were moving inside the breast array coil, we assumed to move the detectors from the isocenter of the RF coil in 10mm steps going from 50mm away from the end of RF coil to 30mm away from the isocenter of the RF coil. Resonance frequency was measured at each position. For MR imaging, a cylindrical shaped phantom (diameter = 90 mm, length = 240 mm) was filled with 2.0±0.05 g/L CuSO4-5H2O, 4.5±0.05 g/L NaCl and 1.89L of distilled water. This phantom was placed into a 4T (170.288MHz) whole-body magnet (Magnex Scientific, Oxford, UK) with a clear bore of 940 mm. The MR pulse sequence parameters were: sequence = 2D gradient echo, slice orientation = coronal, repetition time (TR)/echo time (TE) = 300ms/15ms, flip angle (FA) = 50°, matrix = 256x256, field of view (FOV) = 150mm x 150 mm, slice thickness = 5.0 mm, number of excitations (NEX) = 1.

Fig.3: The rectangular shaped boxes (purple color) were located inside the RF coil. Two boxes faced each other with a 80mm gap. (a) Top view. (b) Oblique view.

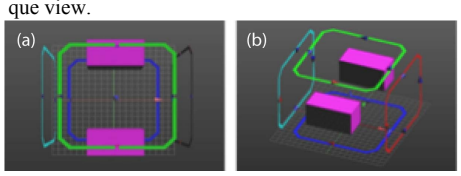


## Results

In the simulation studies the RF shielding box did not cause $H_1$ field distortions but $H_1$ field magnitude was decreased about 0.5dB as shown in Figs 4(c-d). The performance of the actual RF coil was such that the Q-factor and impedance for the top coil frame (channel #1) changed ± 1.95% (Q-factor: 153~159) and ± 1.4% (Impedance: 145~149), respectively while the CZT detectors were moving toward RF coil. In case of the left side of the coil frame (channel #2), Q-factor and impedance changed by ± 2.2% (Q-factor: 136~142) and ± 1.74% (Impedance: 115~119). These results were also observed in the MR experiments. MR Phantom image with the presence of RF shielding boxes was still uniform and the signal to noise ratio (SNR) decreased only by 5.5%. However, when the RF shielding box was in contact with the phantom, the image was distorted due to eddy currents induced in the fine copper fabric shielding from gradient switching as shown in the difference image Fig.5(c).

Fig.4: (a) H1 field without shielding boxes. (b) H1 magnetic field vector without shielding box. (c) H1 field with shielding boxes. (d) H1 magnetic field vector with shielding boxes. These are coronal views from isocenter of RF coil, which are normalized to 2.95e-010 A/m input power.

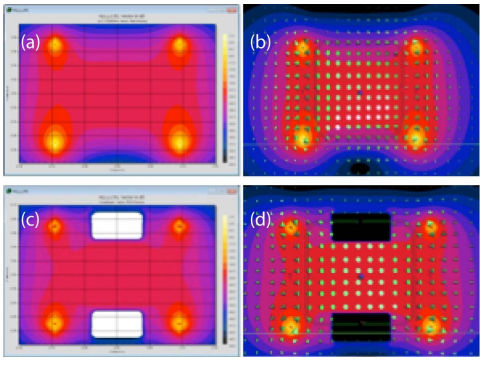


## Discussion and Conclusion

We constructed a four-channel breast array coil, demonstrating the feasibility of a dedicated breast imaging system that combines two different modality systems. The presence of RF shielding box in the four channel breast array coil resulted in an insignificant change in the $H_1$ magnetic field, Q-factor, impedance, and resonance frequency of the RF coil except eddy current distortion. In order to reduce the distortion by eddy current, segmented shielding box should be designed.

Fig.5: Coronal phantom view. (a) Phantom image without shielding boxes. (b) Phantom image with shielding boxes. (c) Subtracted image from (a) to (b).

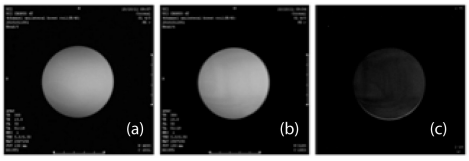


## References

[1] *Lehman CD., et al. N Engl J Med* 356(13): 1295-303 (2007). [2] *Kriege, M., et al. N Engl J Med* 351(5): 427-37 (2004). [3] *Becherer, A., et al. Nucl Med Commun* 18(8): 710-8 (1998).